Posted on Authorea 6 Aug 2020 — The copyright holder is the author/funder. All rights reserved. No reuse without permission. — https://doi.org/10.22541/au.159674586.63598772 — This a preprint and has not been peer reviewed. Data may be preliminary.

# A spatially resolved model for pressure filtration of edible fat slurries

Harry Van den Akker[1], Doedo Hazelhoff Heeres[2], and William Kloek[3]

[1]University of Limerick Faculty of Science and Engineering
[2]Delft University of Technology Faculty Applied Sciences
[3]Royal FrieslandCampina

August 6, 2020

## Abstract

A spatially resolved 1-D pressure filtration model was developed for a slurry of edible fat crystals. The model focuses on the expression step in which a cake is compressed to force the liquid through a filter cloth. The model describes the local oil flow in the shrinking cake modeled as a porous nonlinear elastic medium existing of two phases, viz. porous aggregates and inter-aggregate liquid. Conservation equations lead to a set of two differential equations (vs time and vs a material coordinate ?) for two void ratios, which are solved numerically by exploiting a finite-difference scheme. A simulation with this model results in a spatially resolved cake composition and in the outflow velocity, both as a function of time, as well as the final solid fat contents of the cake. Simulation results for various filtration conditions are compared with experimental data collected in a pilot-plant scale filter press.

## Introduction

Pressure filtration/expression is a process performed in many operations such as dewatering of sludge in waste water treatment [1], thickening of minerals and oil sands tailings in the mining industry [2, 3] and of coal reuse slurries [4], and expressing biological material in the food and beverage industry, such as sugar beet pulp or oil seeds. This paper deals with pressure filtration/expression in a membrane filter press, in which edible fat crystal aggregates, with a diameter of the order of 100 µm (see Figure 1), are separated from an oil-like mother liquor. Essentially, our pressure filtration consists of the same steps as the flexible-membrane plate-and-frame filter press cycle shown in figure 1 of the paper by Stickland et al. [5]. In the application of current interest, a specific pressure-time profile is imposed with the view of optimizing or improving the filtration process in terms of filtration time and the final solid fat contents of the cake.

In a somewhat simplified version of this filtration process, a cake is compressed one-sided to force the liquid through a filter cloth at the other side. At the start of this pressure assisted filtration process, the cake consists of loosely packed porous crystal aggregates containing oil while surrounded by a continuous oil phase (see Figure 2). When the pressure is increased, the cake with the aggregates is compressed to force the oil out of the aggregates and to flow, along with the oil surrounding the aggregates, through the consolidating cake towards the filter cloth at the other end. This paper describes a novel model for describing this 1-D expression process in terms of temporally and spatially resolved porosities of aggregates and cake, resulting in a time-dependent oil flux through the cloth out of the cake.

## Hosted file

`image1.emf` available at https://authorea.com/users/349280/articles/474345-a-spatially-resolved-model-for-pressure-filtration-of-edible-fat-slurries

*Figure 1* - Image of a slurry with spherulitic fat crystal aggregates; the scale in the lower right corner is 100 µm

Posted on Authorea 6 Aug 2020 — The copyright holder is the author/funder. All rights reserved. No reuse without permission. — https://doi.org/10.22541/au.159674586.63598772 — This a preprint and has not been peer reviewed. Data may be preliminary.

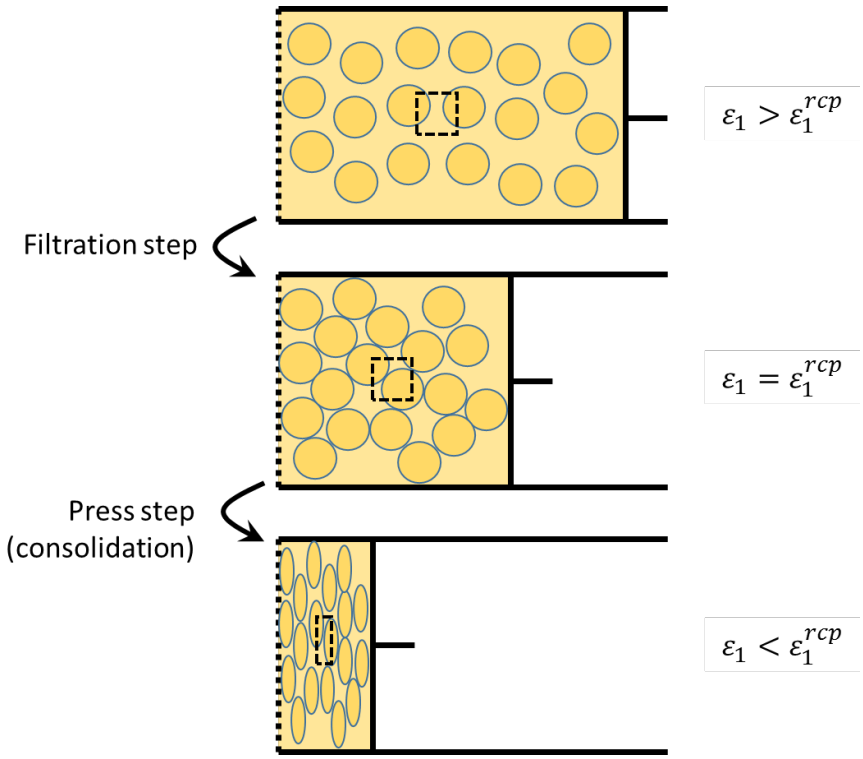


*Figure 2* - The two stages of a filtration and expression process separated by the random close packing (see the middle figure) representing the transition from filtration to expression.

The topic of cake filtration goes back to the paper by D'Arcy, as early as 1856, on the flow of water through sands and sand stones, and was then further investigated in the 1920s and 1930s in papers by Terzaghi [6], Ruth [7] and Carman [8]. Ruth [7] referred to the "widespread idea that the mechanism of filtration is one of such extreme variability that the engineer may perhaps never hope to find law and order in its operation". Since then, the topic has challenged many experimentalists and modelling researchers: the review by Olivier et al. [9] in 2007 already cites 159 papers. An updated review of the topic is beyond the scope of the current paper. We will just focus on our novel expression model and discuss where it differs from earlier models.

The basic filtration equations due to Ruth [7], still in use today, relate filtrate volume as a function of time to pressure drop (over filter cake and filter medium) in terms of specific resistance and volume of the filter cake. Terzaghi [6], interested in consolidation of clay due to a load on top, assumed that layer (or cake) thickness, compressibility and permeability remain constant. Tiller et al. [10] combined Darcy's law for the flow through a porous medium with the notions of solids pressure and consolidation, which not only are relevant to soil mechanics but also to the filter cake of current interest. The common models for constant pressure filtration lead to a quadratic relationship between filtration time and filtrate volume [11, 12]. Stickland et al. [5] reviewed deviations from such a quadratic behaviour. Owolarafe et al. [13] reported about a model for expressing oil from oil palm fruit on the basis of Darcy's law for a cylindrical geometry and supplemented with several empirical relations.

Shirato et al. [14] distinguished between primary consolidation and secondary consolidation (due to creep), releasing the assumption of instantaneous mechanical equilibrium made in the Terzaghi model. Venter et al. [15] successfully applied the Shirato model to the expression behavior of cocoa liquor from finely grinded cocoa nibs. The Shirato model was also used by Abduh et al. [16] for studying the expression of rubber seed oil from dehulled rubber seeds in a hydraulic press. Buttersack [17] developed a two-zone model. In the first zone, with a void fraction between the initial value and a threshold value, the solids-solids interaction is

Posted on Authorea 6 Aug 2020 — The copyright holder is the author/funder. All rights reserved. No reuse without permission. — https://doi.org/10.22541/au.159674586.63598772 — This a preprint and has not been peer reviewed. Data may be preliminary.

ignored. When and where the water content falls short of the threshold value, a second zone consisting of an solids network with increasing elasticity modulus is formed. Filtration and consolidation are not regarded as subsequent stages, but are assumed to occur alongside each other to a extent varying in time. This elastic network may be associated with the dense sphere packing for a filter cake composed of spherical particles. His model gave satisfactory results for press-dewatering of materials such as protein, sawdust, semi-solid clay and sugar-beet tissue.

In an increasingly sophisticated approach, Lanoisellé et al. [18] studied pressure filtration of cellular material (as applied in various agro-food processes) and pointed out that for cellular filter cakes the expression step is much more complex than for mineral cakes. This was already appreciated by Mrema and McNulty [19] who built their model of oil expression from oil seeds upon three elements: (1) the oil flow through the cell wall pores; (2) the oil flow in the inter-kernel voids; and (3) consolidation of the oil seed cake. More or less similarly, Lanoisellé's "Liquid-Containing Biporous Particles Expression Model" describes liquid transport within a network of three different volume fractions of a cake: extra-particle, extracellular and intracellular with different behavior. The resulting system of three complex partial differential equations is solved for a constant imposed pressure and allows for the calculation of the total layer settlement as well as the deformation of the separate extra-particle, extracellular and intracellular volumes. The more recent paper by Petryk and Vorobiev [20] uses a similar model to describe the expression of soft plant materials. However, in both papers, the cellular material properties are very different from those of the fat crystal aggregates of current interest while the pressures applied are much higher than in a filtration process of edible fat crystals.

Kamst et al. [21, 22] modified the old empirical non-linear viscoelastic model due to Nutting (1921) to describe the compressibility of palm oil filter cakes which are highly compressible and viscoelastic. In addition, these authors used a strain hardening model to accommodate the effect of the pressure history of the filter cake. These models, combined with an empirical relation for the permeability, made up a novel expression model. The numerical implementation was done with a finite difference scheme exploiting an exponential grid and a variable time step. This model ignores the Kozeny-Carman equation, just like Tien and Ramarao [23] question the applicability of the Kozeny-Carman equation to consolidating cakes, after Grace already did the same in 1953.

Kamst's expression model predicts a pressure of 4.7 bar above which the solid fat content (SFC) does not increase anymore. Another finding of the Kamst model – relevant for us – was that applying a constant pressure, compared to a time-dependent pressure profile with the same end pressure, does not lead to a higher eventual SFC, although the option of applying different pressure-time profiles was not studied. Further, some of Kamst's experiments and simulations exceed the time scales of our process by an order of magnitude. Most importantly, however, their model ignores the biporous nature of the filter cake (in their case, palm oil), while the double porosity is a very attractive element of Lanoisellé's model, given the fat crystal slurries of current interest.

After filling of a filter chamber (during which some liquid already may leave the chamber), the first step is filtration (see figure 2, top): as long as the inter-aggregate porosity is smaller than the random close packing $\epsilon_{\text{rcp}}$ (=0.64). When pressurization continues, the stage of expression or consolidation is entered in which the aggregates get compressed and squeezed (see figure 2, bottom). The expression model we developed and describe in this paper builds on the above three elements described by Mrema and McNulty [19] and on Lanoisellé's biporous model [18] while considering the typical behaviour and physical properties of the edible fat crystal aggregates of current interest and the pressure levels of the pertinent expression process. The crystal aggregates will therefore be considered as additional sources of oil when squeezed in the expression stage. For the sake of simplicity, we will consider a flat cake with (essentially) 1-D transport of liquid, as a result of a unidirectional pressure applied at the right-hand side of the cake, towards a filter cloth at the left-hand side through which the liquid leaves the cake. We do assume that the agglomerates stay intact, i.e. do not break up when squeezed.

**Some basics**

Posted on Authorea 6 Aug 2020 — The copyright holder is the author/funder. All rights reserved. No reuse without permission. — https://doi.org/10.22541/au.159674586.63598772 — This a preprint and has not been peer reviewed. Data may be preliminary.

The volume reduction of a fat crystal aggregate upon compression, or squeezing, implies the aggregate must release oil, as the intrinsic densities of the oil and fat may be taken constant. On the analogy of Lanoisellé's biporous model [18], we therefore distinguish between the inter-aggregate liquid (surrounding the crystal aggregates) with volume fraction $\epsilon_1$ and the liquid contained inside the aggregates with porosity $\epsilon_2$. We presume that the pores inside the aggregates are smaller than the inter-aggregate pores by at least an order of magnitude. We define the complements of the above liquid volume fractions: the inter-aggregate solidosity (or packing fraction) $s_1 = 1\text{-}\epsilon_1$ , the aggregate solidosity$s_2 = 1\text{-}\ \epsilon_2$ and the total solidosity $s = s_1 s_2$. As very common in filtration and expression paper, we work in terms of void ratios denoting the volume of liquid per volume of solids; in our case, the inter-aggregate void ratio $e_1 = \epsilon_1 / s_1$ and the (intra-)aggregate void ratio $e_2 = \epsilon_2 / s_2$. The latter void ratio denotes the aggregate pore volume per solid fat volume. The total void ratio $e$ denotes the combined volume of intra-aggregate and inter-aggregate liquid per volume of solids. Owing to the above $s = s_1 s_2$ , we can write

All volume fractions, solidosities and void ratios vary spatially and in time. Our model aims at resolving them.

Following e.g., Terzaghi [6], Sørensen et al. [24], Kamst et al. [21] and Landman and White [12], we apply the Lagrangian or material coordinate $\omega$ , defined by

where $x$ denotes the spatial coordinate in the direction of the flow towards the cloth filter, with $x = 0$ at the high-pressure end. This transformation simplifies the equation(s) – see *e.g.* , Smiles [25] – and facilitates the numerical solution. In the material coordinate system, the only flow is that of the liquid relative to the solids. The liquid flux passing the solids is denoted by $u$and is related to the linear liquid and solids velocities by

In exploiting this material coordinate system we deviate from the analyses presented by Lanoisellé et al. [18] and Petryk and Vorobiev [20].

**The expression model**

Due to the distinction between inter-aggregate and intra-aggregate liquid, we need two continuity equations with a source and sink term, respectively, at the RHS. Thanks to the use of the material coordinate$\omega$ , we arrive at simple continuity equations for the inter-aggregate oil

and for the intra-aggregate oil

respectively, in which $q$ in the source/sink terms at the RHSs denotes the release, per aggregate volume (in $s^{-1}$), of inter-aggregate oil from the aggregates. We have dropped the convective term in Eq. (1.4), since as long as the liquid stays within the aggregate pores, its velocity (relative to the solids) is zero. In Eq. (1.4), the total solidosity occurs within the time derivative. Our biporous model essentially differs from the simple single continuity equation *[?]e/[?]t = [?]u/[?]* used by Sørensen et al. [24] and Kamst et al. [21].

The (local) flux $u$ depends on the (local) pressure gradient in the liquid phase and is assumed to obey Darcy's law with permeability$k$ . The convective term of Eq. (1.4) is then rewritten:

The liquid pressure balances the stress in the deforming filter cake (see *e.g.* , Olivier et al. [9]) :

while an elastic modulus $E$ connects the solids pressure$p_s$ with the logarithmic strain:

with $\delta$ standing for the thickness of the filter cake and the subscript 0 denoting initial values, before cake deformation sets in. Applying the chain rule twice, using Eqs. (1.7) and (1.8), and eliminating the total solidosity $s$ results in

We should realize that in a non-linearly elastic medium the elastic modulus depends on the filter cake strain itself, *i.e.* $E = E\ (e_1,\ e_2)$. These manipulations turn the (seemingly) convective term of Eq. (1.4) into a diffusive term. Such a diffusive term is not uncommon: see *e.g.* , Tosun [26], Sørensen et al. [24], Kamst et al. [21], and Olivier et al. [9]. As a matter of fact, the basic idea can already be found in the classical Terzaghi paper dated as early as 1923 [6].

Posted on Authorea 6 Aug 2020 — The copyright holder is the author/funder. All rights reserved. No reuse without permission. — https://doi.org/10.22541/au.159674586.63598772 — This a preprint and has not been peer reviewed. Data may be preliminary.

Substituting Eq. (1.9) into Eq. (1.4) and re-writing the solidosities $s$ and $s_2$ in terms of $e_1$ and $e_2$ results in

while Eq. (1.5) can be rewritten as

The next step is to find an expression for the release rate $q$ . Different from Mrema and McNulty [19], we assume the flux out of the aggregates is Darcian, with a permeability $k_2 = k_2(e_2)$ associated with the aggregates, through the specific area $a = 6/d_a$ for the spherulitic aggregates of constant average size $d_a$ . The pressure gradient can be transformed as above, resulting in

The above Eqs. (1.10) and (1.12) contain the cake properties $k_1$, $k_2$ and $E$ which all are dependent on the pertinent the pertinent void ratios. We need empirical correlations for these parameters. As, according to Tien and Ramarao [23], the Kozeny-Carman relation is not valid under consolidating conditions, we use the Meyer and Smith [27] correlation

For $k_1$, we use void ratio $e_1$ and aggregate size $d_a$ , while $k_2$ needs $e_2$ and the typical diameter $d_c$ of the individual crystals that build the agglomerate. Fitting an exponential function through data for strain measured at varying constant load $p_p$ results in an expression of the type

Using Eq. (1.8) then results in the expression

The eventual set of the two partial differential equations for $e_1$ and $e_2$ then is

in which

$C_e$ is a type of diffusion coefficient, in the consolidation literature denoted as a modified consolidation coefficient [9, 24]. While this coefficient in a real-life expression process is varying with position and in time, in many papers (*e.g.* , [14], [28]) it is treated as a constant: this simplifies solving the consolidation equation which is a second-order partial differential equation. Kamst et al. [21], however, appreciate the consolidation coefficient (also) depends on local cake porosity and compressibility. The review paper by Olivier et al. [9] cites a number of authors (among which [5]) who all use similar relationships for diffusivity or consolidation coefficient. Our expression for $C_e$ in Eq. (1.18) is essentially different from earlier proposals due to the biporous character of our fat crystal slurry as a result of which it includes both the intra-aggregate and the inter-aggregate solidosities. In addition, our consolidation equation, Eq. (1.16), contains a source term which to the best of our knowledge is a novelty. Finally, our model looks much simpler than Lanoisellé's.

In more general terms, our expression model is a rheological model composed of two dashpots in series parallel to a spring. The double porous nature of the fat crystal aggregate filter cake is represented as a series of two dashpots described with the Meyer & Smith correlation for the permeability (rather than the Kozeny-Carman relation). The spring is due to the elastic modulus that can be determined experimentally with a constant load test.

**Boundary and initial conditions**

Solving the set of Eqs. (1.16) – (1.17) requires initial and boundary conditions for $e_1$ and $e_2$. The material coordinate system, see Eq. (1.2), used in the expression model is illustrated in Figure 3. With this $\omega$ -coordinate, both boundaries are stationary. The position of the cloth at $\omega = 0$ is denoted by $\Gamma_1$, while that of the piston at $\omega = \Omega$ is denoted by $\Gamma_2$.

Posted on Authorea 6 Aug 2020 — The copyright holder is the author/funder. All rights reserved. No reuse without permission. — https://doi.org/10.22541/au.159674586.63598772 — This a preprint and has not been peer reviewed. Data may be preliminary.

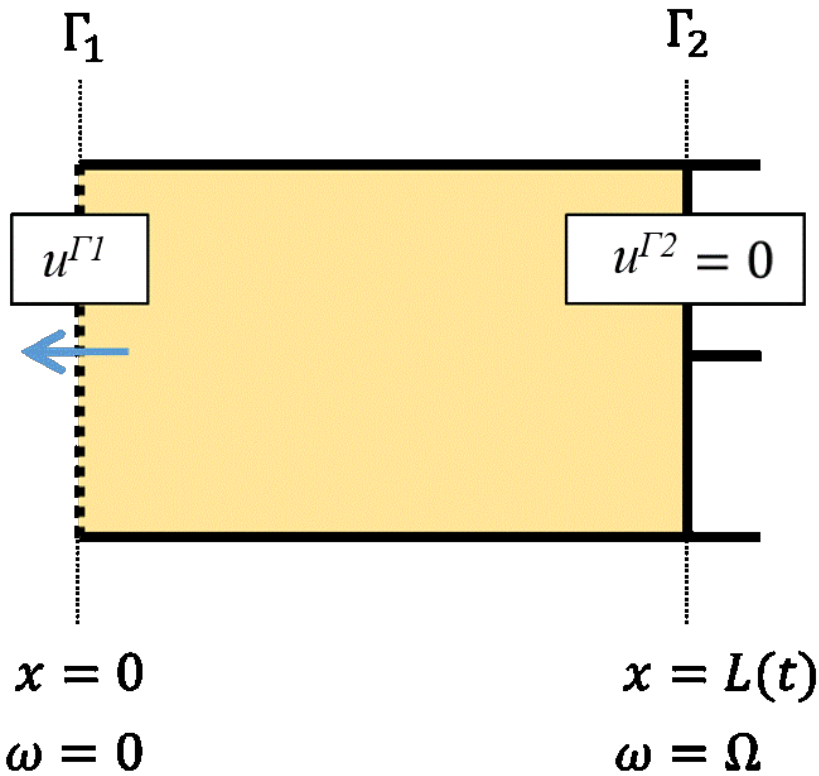


*Figure 3* - The domain of the expression with the cloth filter (taken infinitely thin) at the LHS and the pressure piston at the RHS, plus the notation and the two coordinate systems

At $\Gamma_2$ , the liquid flux $u$ always equals zero, implying that , thanks to Darcy's law, and therefore, as in Eq. (1.12):

A similar Neumann boundary condition for $u$ is applied at$\Gamma_1$ during the rest mode after the filling has been completed, resulting in similar boundary equation for$e_1$ at $\Gamma_1$ as Eq. (1.20). With the view of the boundary condition for $e_1$ at$\Gamma_1$ during the filling mode and the pressing mode, we use Eq. (1.1) to find

We then need values for $e_2$ and $e$ at$\Gamma_1$, and to calculate $e$ , given Eqs. (1.8) and (1.14), also values for the strain $\epsilon_{\lambda_\varsigma}$ and the pressure at $\Gamma_1$ . For the latter, we need the pressure drop $\Delta\pi_\varsigma$ over the cake which due to Darcy's law relates to the piston pressure $p_p$applied at $\Gamma_2$ :

in which $R_f$ denotes the flow resistance of the filter cloth and $R_c$ that of the cake which follows from

The void ratio $e_2$ is a function of time only and therefore we need just an initial value for $e_2$for the whole domain:

withdenoting the solid fat volume fraction at random close packing. The initial condition for $e_1$ runs as

Finally, the total void ratio $e_0$ of the porous medium at the start of the expression step, needed in Eqs. (1.18) and (1.19), is related to according to

**Numerical implementation**

With the view of solving the two partial differential equations (1.16) and (1.17) numerically, the 1-D domain [0, Ω] (σεε Φιγυρε 3) ις δισςρετιζεδ ιντο Θ+1 νοδες νυμβερεδ ωιτη συπερσςριπτ $\vartheta$ . Εερψ νοδε $\omega^\vartheta$ is assigned a length interval [$\omega^\vartheta$ -$\frac{1}{2}\Delta\omega$ , $\omega^\vartheta$ +$\frac{1}{2}\Delta\omega$ ], with $\Delta\omega = \Omega$ /J. Half of the length interval associated with each

of the two boundary nodes is inside the domain [0, Ω]. Το αλλοω φορ ιμποσινγ τηε αβοε βουνδαρψ ςονδιτιονς, ονε γηοστ νοδε ις αδδεδ ατ ειτηερ σιδε οφ τηε δομαιν, ωιτη ινδιςες $\vartheta$ =1 ανδ $\vartheta$ =Θ+3, συςη τηατ τηε πλανε $\omega$ =0 is in $\omega$ $^{2}$ and the plane $\omega = \Omega$ is in$\omega$ $^{J+2.}$

The equations are solved with an Euler-forward finite-difference scheme implemented with MATLAB R2014b. To impose numerical stability in our explicit scheme, the time step $\Delta t$ should obey the criterion

where $Fo$ $_{\Delta}$ is a local Fourier number and$C_e$ $_0$ is a constant much larger than the maximum value of the consolidation coefficient$C_e$ of Eq. (1.18), *i.e.*$C_e$ $_0$ should be much larger than the constant factor in Eq. (118).

The discretisation of Eqs. (1.16) and (1.17) is pretty straightforward. The same applies to the boundary conditions, except that for, calculating a value of $e$ $_2$ at node$\omega$ $^{2}$ (i.e., at $\omega$ =0) from Eqs. (1.17) and (1.19), a value of $e$ $_1$ is needed at ghost node$\omega$ $^{1}$. It is found by extrapolating from the$e$ $_1$ values at nodes $\omega$ $^{2}$,$\omega$ $^{3}$and $\omega$ $^{4}$ by using equal ratios of differences between these nodes, given that the$e$ $_1$ profile is found to be square root shaped. Care must be taken that the $e$ $_1$ values at nodes$\omega$ $^{1}$ should not become negative. To realize the Neumann boundary condition at $\omega = \Omega$ by applying a central differencing scheme to Eq. (1.20), the value of$e$ $_1$ at node $J$ +3 is taken equal to that at node $J$ +1. More details can be found in Hazelhoff Heeres' MSc thesis [29].

The time dependent filter cake thickness is calculated with

in which the superscript $i$ denotes the time step of a variable and =1 unless $j$ =2 or $j$ =$J$ +2: then it is $\frac{1}{2}$.

The outflow velocity through the filter cloth then follows from

**Experiments**

Of course, the above expression model was calibrated and validated by means of experimental results collected at pilot plant scale in a relatively small membrane filter press. It contained five filter plates making 4 filter chambers, each with 2 cross-flow areas of about 40 cm x 40 cm, creating 3 cm wide filter chambers. The flow resistance of the filter cloth was half a mm in thickness and made out of polypropylene. The edible fat crystal aggregate slurry was prepared in an on-site crystallizer and then pumped by a slurry pump into the filter chambers. The liquid produced during the expression process was collected in a bin standing on an electronic balance to register the flow rate.

| Test # | Rate of pressure increase, bar/min | Number of pressure steps | Duration of expression step, min |
|---|---|---|---|
| 1 | 1 | 1 | 10.5 |
| 2 | 0.5 | 1 | 15.2 |
| 3 | 1 | 3 | 13.5 |
| 4 | 1 | 3 | 11.8 |
| 5 | 1Q-sine | | 14.9 |

*Table 1* – Summary of experimental conditions of 5 test runs for validation and calibration of the expression model. The final pressure was the same in all 5 cases. In the tests with 3 pressure steps, pressure was held constant for a few minutes after each increase of 1 bar/min.; 1Q-sine means a pressure *vs* time profile having the shape of a quarter of a sine.

Typically, some 20 kg of liquid was produced per experiment; depending on the manually controlled pressure profile imposed (rate of pressure increase, number of steps, duration of maximum pressure), this took between 10 and 15 minutes, the final maximum pressure in all cases being of the order of 5 bar(g) during some 5 minutes. Table 1 summarises the conditions of 5 test runs all done on different days: tests #1 and #2 with a different edible fat batch than tests #3, #4 and #5. Figure 4 presents two pictures of filter cakes produced in the test rig. The final solid fat content of the cake was measured with a NMR analyser. For the sake of our simulations, we take the (measured) solid fat content (which is on a mass basis) equal to the total



Posted on Authorea 6 Aug 2020 — The copyright holder is the author/funder. All rights reserved. No reuse without permission. — https://doi.org/10.22541/au.159674586.63598772 — This a preprint and has not been peer reviewed. Data may be preliminary.

solidosity in our model (which is on a volumetric basis) due to ignoring density differences between oil and (liquid) fat.

### Hosted file

`image40.emf` available at https://authorea.com/users/349280/articles/474345-a-spatially-resolved-model-for-pressure-filtration-of-edible-fat-slurries

*Figure 4* - Top view and side view of filter cakes produced in the pilot plant filter press. The membrane side is up. The thickness of the cakes is almost 25 mm.

### Calibration of the model

A straightforward validation of model predictions by means of experimental data collected in these tests is hampered by several experimental technicalities. First of all, as the model is 1-D, it presumes a uniform composition of the medium in the other two directions and it ignores fluid motion and mixing, which certainly is not the case during the filling stage. A combined filtration and consolidation process already starts spontaneously during the filling of the filter chambers without any pressure being imposed. The simulation of the expression starts as soon as in the filling stage the inter-aggregate porosity $\epsilon_1$ falls below at the random close packing when the agglomerates start feeling they get compressed. In the tests, the filling is followed by a waiting period of some 20 s before the pressure is applied. In the simulations, this waiting period, or rest mode, is realized by imposing a zero outflow at $\Gamma_1$. Then, pressure is applied and expression resumes resulting in a continued outflow. Another awkward technicality is that in the tests the separated liquid is staying behind in the tubing and piping between filter and collecting bin, while also the residence time in the collecting system leading to a retarded response of the balance is not in the model. A perfect match between model simulation and experiment is therefore not to be expected. We therefore carried out a calibration step first.

Table 2 presents model constants, physical properties, dimensions and simulation parameters used in both the calibration study and the validation study. The number of intervals J was selected after a sensitivity analysis with the view of balancing computational burden and accuracy. The flow resistance $R_f$ of the filter cloth had been measured separately by filtering oil without solid fat. The solidosity $s^{rcp}$ at random close packing was obtained by measuring the solid fat content of a cake in centrifugation experiments. The initial value $e_0$ follows from $s^{rcp}$ thanks to Eq. (1.26). In its turn, $e_0$ is used in estimating $C_{e\,0}$ with Eq. (1.18). The initial thickness $L_0$ of the filter cake was set to 2.05 cm in an attempt to correct for the loss of liquid in the first phase of the filling stage when there was outflow without pressure being applied. Then, Eq. (1.2) was used to calculate $\Omega$ with $s^{rcp} = 0.228$ as found in our experiments.

However, the model contains three more parameters we actually do not know from the onset, *viz.* the aggregate diameter $d_a$ occurring in Eqs. (1.18) and (1.19), the inter-aggregate solidosity at random close packing needed to calculate the initial values $e_{1,0}$ and $e_{2,0}$ with Eqs. (1.24) and (1.25), and the solid fat content, or total solidosity $s$, at the start of the expression process.

| Quantity | Value | Units | Equation |
|---|---|---|---|
| $c_1$ | 33.1 | mPa | 1.14 |
| $c_2$ | 5.18 | - | 1.14 |
| $C_{e0}$ | $10^{-5}$ | $m^2/s$ | 1.27 |
| $\rho$ | 910 | $kg/m^3$ | |
| $\mu$ | 0.06 | $Ns/m^2$ | |
| $d_c$ | 2 | µm | 1.19 |
| $R_f$ | $1.6 \cdot 10^{-9}$ | $m^{-1}$ | 1.22 |
| $L_0$ | 2.05 | cm | |
| $s^{rcp}$ | 0.228 | | 1.24 |



Posted on Authorea 6 Aug 2020 — The copyright holder is the author/funder. All rights reserved. No reuse without permission. — https://doi.org/10.22541/au.159674586.63598772 — This a preprint and has not been peer reviewed. Data may be preliminary.

| Quantity | Value | Units | Equation |
|---|---|---|---|
| $\Omega$ | 0.467 | cm | 1.2 |
| J | 23 | - | |
| $\Delta\omega$ | 0.203 | mm | |
| $\Delta t$ | 2.1 | ms | 1.27 |

*Table 2* - Summary of parameters used in the simulations with the expression model

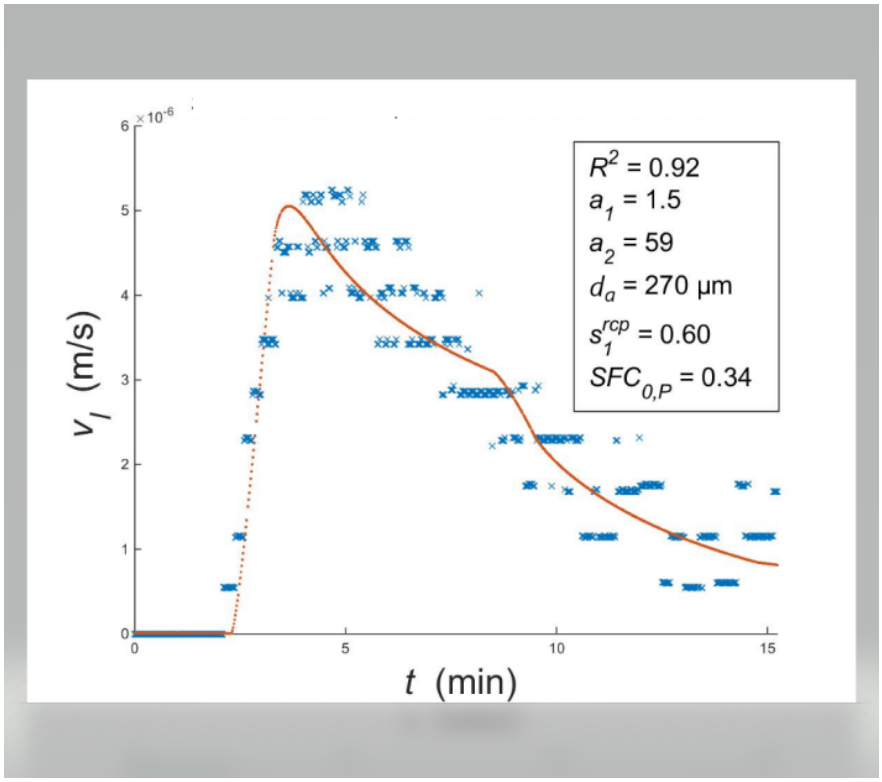


*Figure 5* – Comparison of simulated (red line) and experimental (blue crosses) outflow velocities in test #1 (left) and test #2 (right) where the simulations were calibrated by use of optimised values for the five parameters mentioned in the legends.

In addition, it turns out that, even with reasonable guesses for these three parameters, the outflow velocity calculated with Eq. (1.29) cannot be made to match the outflow as measured in the tests. The way out was to introduce two so-called flow resistance factors, denoted by $a_1$ and $a_2$, with the view of reducing the values of consolidation coefficient $C_e$ and release rate $q$, see Eqs. (1.18) and (1.19), by dividing them by $a_1$ and $a_2$, respectively. Tests 1 and 2 were then used to calibrate the expression model by systematically varying the above five parameters within physically plausible ranges. Figure 5 presents for these two tests the comparison between simulated and experimental outflows as a function of time. The legends also show the $R^2$ values which indicate a match which per test is very good.

The two sets of optimised coefficients differ quite a bit, while the only difference between the two tests is in the rate of pressure increase. The discrepancies between the two sets may illustrate the challenge of dealing with the experimental technicalities. The best thing to do was to average the two sets to produce the following set which will be used for the remainder of the tests of this paper:



Posted on Authorea 6 Aug 2020 — The copyright holder is the author/funder. All rights reserved. No reuse without permission. — https://doi.org/10.22541/au.159674586.63598772 — This a preprint and has not been peer reviewed. Data may be preliminary.

The flow resistance factor $a_1 = 2.7$ may be related to an over-prediction of cake permeability $k_1$ by Eq. (1.13): our own experiments showed an over-prediction by a factor of 5. This also affects consolidation coefficient, see Eq. (1.18). The value 42 for the flow resistance factor $a_2$ may be due an over-estimation of both agglomerate permeability $k_2$ and crystal diameter $d_c$ (which occurs squared). The value 0.59 for the inter-aggregate solidosity looks a bit low, where Torquato et al. [30], in a molecular dynamics study of hard spheres, report a packing fraction of 0.64 for a maximally random jammed state. Figure 6 shows a comparison of simulation results obtained with the set of optimised coefficients of Eq. (1.30) and experimental outflow velocities for the same tests #1 and #2 as above. Compared to Figure 5, the agreement is less good, with decrease values for $R^2$.

**Hosted file**

`image46.emf` available at https://authorea.com/users/349280/articles/474345-a-spatially-resolved-model-for-pressure-filtration-of-edible-fat-slurries

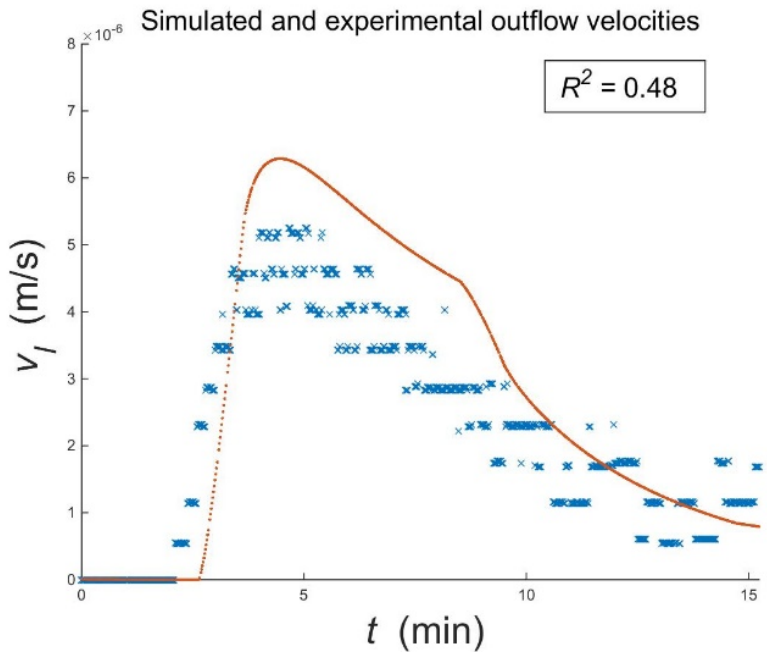


*Figure 6* - Comparison of simulated (red line) and experimental (blue crosses) outflow velocities in test #1 (left) and test #2 (right) where the simulations were calibrated by use of the averaged optimised values for the five parameters mentioned in Eq. (1.30).

**Validation of the model**

The other three tests of Table 1, carried out with a different edible fat batch, were used for validating the expression model including the coefficient of Eq. (1.30). The results for the outflow velocity profiles are shown in Figure 7. Tests 3 and 4 are just duplicates, with an identical simulated velocity profile, although test #4 was stopped earlier than #3, and again show the spread in experimental results due to the technicalities described above. In addition, the manual control of the pressure profile adds to the spread. Note that in both tests #3 and #4, the pressure increase was interrupted twice (see Table 1), the first time at the rather low pressure of 1 bar(g) that was maintained for a few minutes; in the simulations this obviously did not result in an outflow. The agreement between simulation and test is far better again in test #5 where, just like in tests #1 and #2, pressure was increased continuously (though in an different way) up to the same final maximum pressure.



Posted on Authorea 6 Aug 2020 — The copyright holder is the author/funder. All rights reserved. No reuse without permission. — https://doi.org/10.22541/au.159674586.63598772 — This a preprint and has not been peer reviewed. Data may be preliminary.

Posted on Authorea 6 Aug 2020 — The copyright holder is the author/funder. All rights reserved. No reuse without permission. — https://doi.org/10.22541/au.159674586.63598772 — This a preprint and has not been peer reviewed. Data may be preliminary.

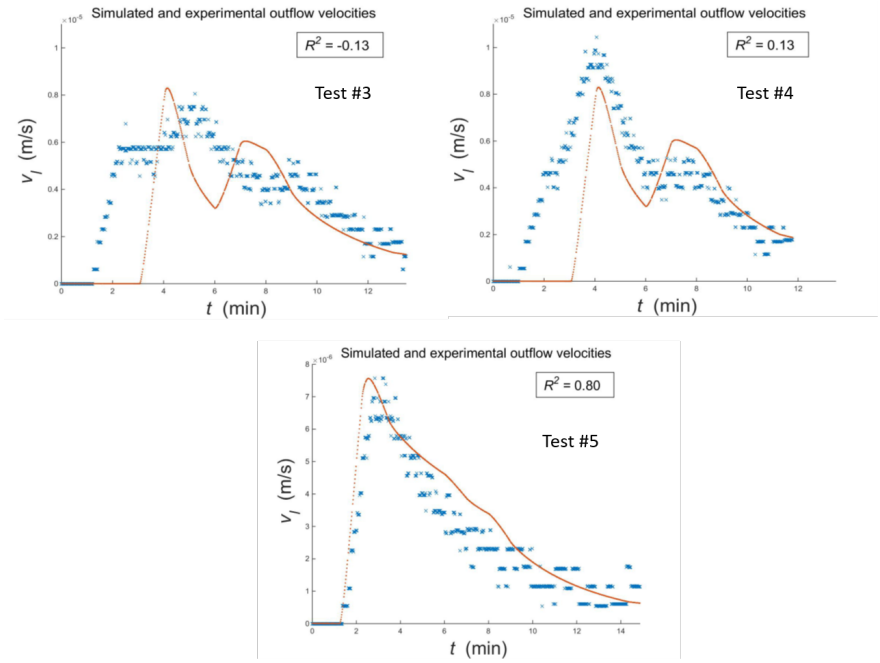


*Figure 7* - Comparison of simulated (red line) and experimental (blue crosses) outflow velocities in tests #3, #4 and #5, simulations having been run with the five optimised parameters mentioned in Eq. (1.30).

**Filter cake composition and profile**

Given the satisfactory results of the calibration study, which was restricted to the outflow velocity through the membrane, we now present the model's findings with respect to the

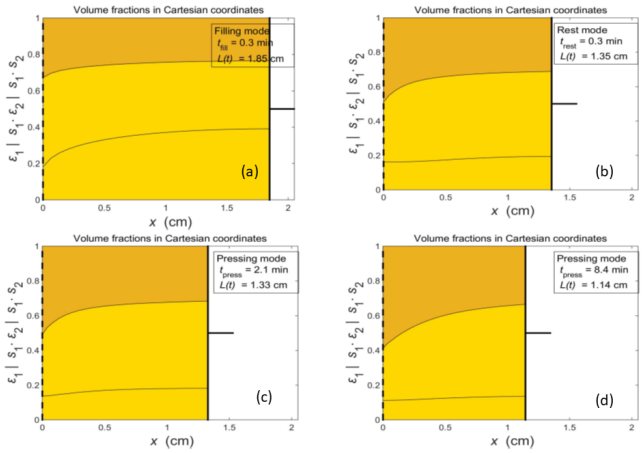


*Figure 8* - Volume fractions *vs* position in the cake as calculated by our model with the set of coefficients of Eq. (1.30) for test #1. The position of the filter cloth on the left is fixed. The total thickness of the filter cake decreases over time. The lower surface represents $\epsilon_1$ (the inter-agglomerate liquid), the middle one $\epsilon_2 s_1$ (the intra-agglomerate liquid) and the upper one is total solidosity $s_2 s_1$ ($=s$). The times $t_{\text{fill}}$, $t_{\text{rest}}$ and $t_{\text{press}}$ denote the times passed since the start of the filling, rest, and pressing modes, respectively.

spatial and temporal evolution of the filter cake composition which lies at the basis of the outflow velocity. Figure 8 presents a typical result, for test #1, in terms of the volume fractions $\epsilon_1$ (the inter-agglomerate liquid) and $\epsilon_2 s_1$ (the intra-agglomerate liquid) and the total solidosity $s_2 s_1$ ($=s$). Each of these three volume fractions which add up to unity, has been coloured with a different shade of ochre. Each panel of Figure 8 shows, for a specific moment in time, the composition of the cake as a function of $x$ (translated from $\omega$). The upper curves in the four panels exhibit the typical propagating error function shape associated with transient diffusion, with penetration time of the order of 0.2 min (*viz.* ,), while three of the four lower, $\epsilon_1$, curves are rather flat, indicating the release of fat from the agglomerates is rate limiting for the fat separation through the filter cloth. This is due to the second-order diffusion equation for $e_1$ while $e_2$ obeys a simple mass balance. The total thickness of the filter cake decreases over time as indicated by the position of the piston. This decrease clearly slows down as permeability decreases over time, see Eq. (1.13), while the elastic modulus increases, see Eq. (1.15).

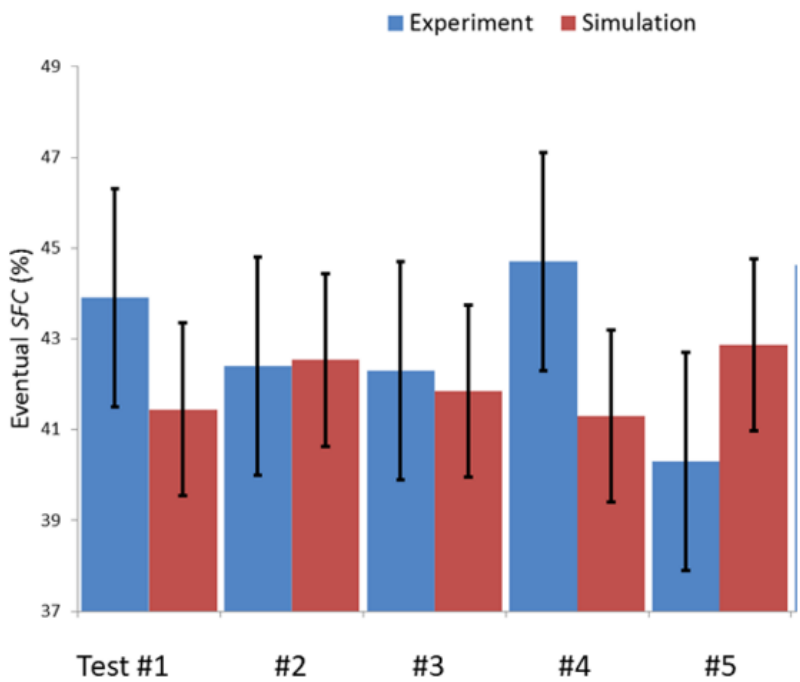


*Figure 9* – Final solid fat content for all 5 cases: comparison between experiment (blue, left) and simulation (purple, right).

Figure 9 illustrates that the (average) eventual solid fat content found in the simulations is in very good agreement with the experimental data, certainly given the uncertainty (represented by the error bars) in both experiments and simulations. The error bars of the simulations are based on differences found in simulations with different sets of calibration coefficients, such as in Figures 5 and 6. The experimental uncertainty is once more clear from the different values of the solid fat content of the similar tests #3 and #4: test #4 was stopped earlier than #3 and therefore should contain more oil indeed (as in the simulations), while this was not observed in the tests. In test #5, the average solid fat content was predicted too high while the outflow simulation (see Figure 7) was very well predicted.

Finally, we checked whether the simulation reproduces the solid fat profile in the eventual filter cake as found in the pilot-plant tests. To this end, the filter cake produced in test #2 was removed from the filter



Posted on Authorea 6 Aug 2020 — The copyright holder is the author/funder. All rights reserved. No reuse without permission. — https://doi.org/10.22541/au.159674586.63598772 — This a preprint and has not been peer reviewed. Data may be preliminary.

Posted on Authorea 6 Aug 2020 — The copyright holder is the author/funder. All rights reserved. No reuse without permission. — https://doi.org/10.22541/au.159674586.63598772 — This a preprint and has not been peer reviewed. Data may be preliminary.

chamber and sliced with the help of an egg slicer into five layers of approximately equal thickness. This is a tedious operation, as oil dripped on the cake during removal and cutting was difficult, with the cake easily crumbling and melting during handling. The solid fat content of ten samples out of each slice was measured and averaged to construct

**Hosted file**

`image52.emf` available at https://authorea.com/users/349280/articles/474345-a-spatially-resolved-model-for-pressure-filtration-of-edible-fat-slurries

*Figure 10* - The final solid fat content in test #2 as a function of position in the filter cake. The five triangles denote the simulation results, while the test results are represented by the overlapping symbols. The uncertainty in the simulation data has been estimated from a number of simulations with varying calibration coefficients.

a profile of solid fat content versus position in the cake. Something similar, though for three slices, was done after completion of the pertinent simulation. In the tests in the membrane filter press, the cake was contained between two membranes, while in the simulation there was just a single membrane (at the left-hand side). For the sake of the comparison in Figure 10 the computed profile was mirrored. As expected, the solid fat concentration is minimum in the middle of the cake in both test and simulation. Note that the final thicknesses of the cake in the test (24.3mm) and in the mirrored simulation (2 x 11.4mm) are not exactly the same, since – due to the technicalities mentioned earlier with respect to the start of the expression stage – also the initial cake thicknesses were taken different. Given the experimental inaccuracies and the simplifications of the 1-D model, the difference between the two curves is surprisingly good.

**Application of the model**

The interest of companies is in producing a high edible fat content in a period as short as possible. This translates into questions as to which final pressure level, which pressure-time profile (including the option of increasing pressure in steps) and which duration of the process are optimum. The expression model reported in this paper could be helpful in deciding on these issues. To illustrate the potential of the model, we investigated the effect of varying the constant rate of pressure increase on the eventual solid fat content, the final pressure level being kept the same.

Figure 11 illustrates, for various rates of pressure increase, how solid fat content increases in time due to a decrease in $e_2$ denoting pore volume (or aggregate oil) per solid fat volume which is constant over time. Eqs. (1.11) and (1.12) tell us that the decrease in $e_2$ depends on the gradient in $e_1$. A slower pressure increase implies that it takes longer for the gradient in $e_1$ to vanish and for the filter cake to obtain an equilibrium state. It also takes longer to reach the final pressure level partly because the squeezing and the oil separation set in later in time, but it results in a higher solid fat content (some 2%). In spite of the limitations and uncertainties of our 1-D filtration model, these results at least suggest our model may successfully be used for ranking process options. We like to emphasize that our experience with tests in a pilot-plant scale membrane filter press suggest that such a ranking exercise is harder, and more expensive, on the basis of tests, due to inevitable slight variations between tests in slurry composition and properties, a range of equipment and operational issues discussed earlier, and the relatively large uncertainties in the measurements.

**Hosted file**

`image53.emf` available at https://authorea.com/users/349280/articles/474345-a-spatially-resolved-model-for-pressure-filtration-of-edible-fat-slurries

Posted on Authorea 6 Aug 2020 — The copyright holder is the author/funder. All rights reserved. No reuse without permission. — https://doi.org/10.22541/au.159674586.63598772 — This a preprint and has not been peer reviewed. Data may be preliminary.

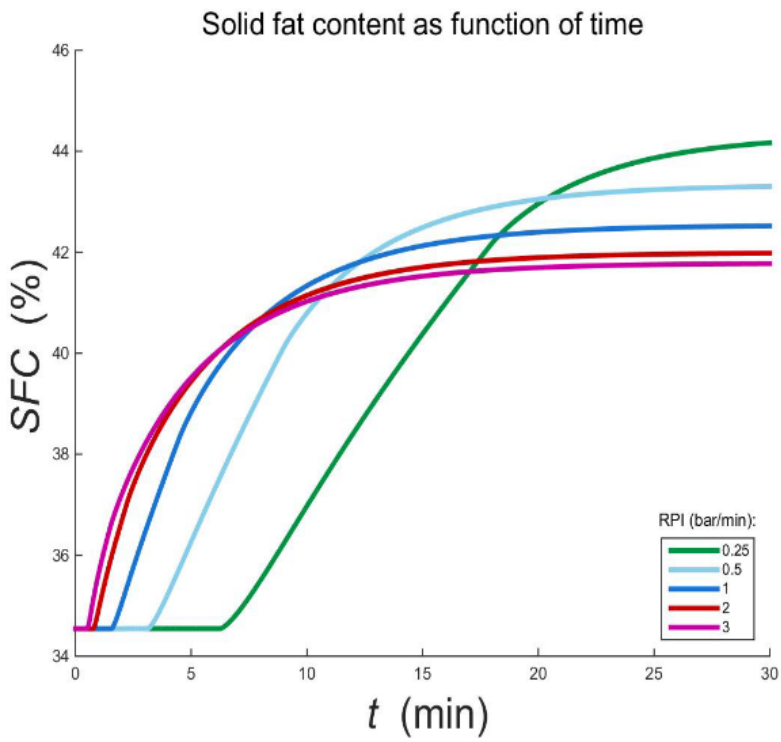


*Figure 11* – Solid fat content (*SFC* , left) and pore volume per solid fat volume (right) as a function of expression time, for various RPIs (rates of pressure increase) in the range 0.25 – 3 bar/min.

**Conclusions**

A 1-D pressure filtration model for edible fats, focusing on the expression step, has been developed and described. The model comprises two differential equations one of which is a second-order diffusion equation with a non-constant consolidation coefficient while the second is a simple transient mass balance. The expression we derived for this consolidation (or diffusion) coefficient is essentially different from earlier proposals in the literature since we explicitly take the biporous character of our fat crystal slurry into account, in terms of intra-aggregate and inter-aggregate solidosities. In addition, our consolidation equation contains a source term which to the best of our knowledge is a novelty. In general terms, our set of two differential equations represents a rheological model composed of a series of two dashpots parallel to a spring. The double porous nature of the fat crystal aggregate filter cake can be conceived as a series of two dashpots described with the Meyer & Smith correlation for the permeability (rather than the Kozeny-Carman relation). The spring is due to the elastic modulus that can be determined experimentally with a constant load test.

The model was implemented in MATLAB with five unknown coefficients remaining, which were calibrated with the help of measured oil outflow rates in two filtration tests in a pilot scale membrane filter press. The model was then validated by using experimental data from five filtration tests. The model is capable of displaying porosities and solidosities, the solid fat content inclusively, as a function of time and of position in the filter cake. In addition, it can generate plots of overall features of the filtration process such as oil outflow velocity, solid fat content of the filter cake and aggregate oil volume, all as a function of time.

The overall conclusion is that the model gives very promising results, qualitatively realistic and obviously pretty reliable, with room for improvement in quantitative respect. Our simulations may also result in process information which is more consistent than data from pilot plant tests which suffer from several equipment technicalities and operational issues. Specific experiments may be helpful to find more reliable

Posted on Authorea 6 Aug 2020 — The copyright holder is the author/funder. All rights reserved. No reuse without permission. — https://doi.org/10.22541/au.159674586.63598772 — This a preprint and has not been peer reviewed. Data may be preliminary.

and accurate data for some cake features such as permeability and elasticity as a function of particularly aggregate properties of typical edible fats.

Finally, the model has been shown to have the potential of exploring the effect of typical process operation variables on eventual solid fat content of the filter cake, such as the rate of pressure increase and, related, the duration of the expression phase.

**Acknowledgments**

The challenge of developing a better expression model was given to a team of PhD students from Dutch Physics Departments in the context of a week-long Physics for Industry event organized by the Dutch research foundation FOM in Fall 2015. The arrangements made by FOM are highly appreciated. In this week, the basis was laid for the model described in this paper which resulted from the MSc final year research project of the second author. The authors acknowledge the practical guidance in lab and pilot plant trials by Richard van Leeuwen, Johan Draisma and Hanung Sonneveld, all FrieslandCampina.

**Literature Cited**

1. LaHeij, E.J., et al., *Fundamental aspects of sludge filtration and expression.* Water Research, 1996. **30** (3): p. 697-703.

2. Xu, Y.M., T. Dabros, and J.M. Kan, *Filterability of oil sands tailings.* Process Safety and Environmental Protection, 2008.**86** (B4): p. 268-276.

3. Angle, C.W., B. Clarke, and T. Dabros, *Dewatering kinetics and viscoelastic properties of kaolin as tailings model under compressive pressures.* Chemical Engineering Research & Design, 2017. **118** : p. 286-293.

4. Raman, G.S.S. and M.S. Klima, *Evaluation of Pressure Filtration of Coal Refuse Slurry: A Fractional Factorial Design Approach.*International Journal of Coal Preparation and Utilization, 2019.**39** (6): p. 332-344.

5. Stickland, A.D., R.G. De Kretser, and P.J. Scales,*Nontraditional constant pressure filtration behavior.* AIChE Journal, 2005. **51** (9): p. 2481-2488.

6. Terzaghi, K., *Die Berechnung der Durchlassigkeitsziffer des Tones aus Dem Verlauf der Hydrodynamischen Spannungserscheinungen (A method of calculating the coefficient of permeability of clay from the variation of hydrodynamic stress with time).* Akademie der Wissenschaften in Wien, Mathematisch-Naturwissenschaftliche Klasse, 1923. **132** : p. 125-138 - see also: Proc. Instn. Civil Engrs. Geotech. Engng., 1995, 113, 191-205.

7. Ruth, B.F., *Studies in Filtration III. Derivation of general filtration equations.* Industrial & Engineering Chemistry, 1935.**27** : p. 708-723.

8. Carman, P.C., *Fluid flow through granular beds.* Trans IChemE, 1937. **15** : p. 150-166.

9. Olivier, J., J. Vaxelaire, and E. Vorobiev, *Modelling of cake filtration: An overview.* Separation Science and Technology, 2007.**42** (8): p. 1667-1700.

10. Tiller, F.M. and H.R. Cooper, *The role of porosity in filtration. 4. Constant pressure filtration.* AIChE Journal, 1960.**6** (4): p. 595-601.

11. Tiller, F.M. and M. Shirato, *The role of porosity in filtration 6. New definition of filtration resistance* AIChE Journal, 1964. **10** (1): p. 61-67.

12. Landman, K.A. and L.R. White, *Predicting filtration time and maximizing throughput in a pressure filter.* AIChE Journal, 1997.**43** (12): p. 3147-3160.

13. Owolarafe, O.K., et al., *Mathematical modelling and simulation of the hydraulic expression of oil from oil palm fruit.* Biosystems Engineering, 2008. **101** (3): p. 331-340.

Posted on Authorea 6 Aug 2020 — The copyright holder is the author/funder. All rights reserved. No reuse without permission. — https://doi.org/10.22541/au.159674586.63598772 — This a preprint and has not been peer reviewed. Data may be preliminary.

14. Shirato, M., et al., *Fundamental studies of expression under variable pressure* Journal of Chemical Engineering of Japan, 1970.**3** (1): p. 105-112.

15. Venter, M.J., N.J.M. Kuipers, and A.B. de Haan, *Modelling and experimental evaluation of high-pressure expression of cocoa nibs.*Journal of Food Engineering, 2007. **80** (4): p. 1157-1170.

16. Abduh, M.Y., et al., *Experimental and modelling studies on the solvent assisted hydraulic pressing of dehulled rubber seeds.*Industrial Crops and Products, 2016. **92** : p. 67-76.

17. Buttersack, C., *2-Zone model for solid-liquid separation by filtration and expression.* Chemical Engineering Science, 1994.**49** (8): p. 1145-1160.

18. Lanoiselle, J.L., et al., *Modeling of solid/liquid expression for cellular materials.* AIChE Journal, 1996. **42** (7): p. 2057-2068.

19. Mrema, G.C. and P.B. McNulty, *Mathematical model of mechanical oil expression from oilseeds.* Journal of Agricultural Engineering Research, 1985. **31** (4): p. 361-370.

20. Petryk, M. and E. Vorobiev, *Numerical and Analytical Modeling of Solid-Liquid Expression from Soft Plant Materials.* AIChE Journal, 2013. **59** (12): p. 4762-4771.

21. Kamst, G.F., O.S.L. Bruinsma, and J. de Graauw, *Permeability of filter cakes of palm oil in relation to mechanical expression.* AIChE Journal, 1997. **43** (3): p. 673-680.

22. Kamst, G.F., O.S.L. Bruinsma, and J. de Graauw, *Solid-phase creep during the expression of palm-oil filter cakes.* AIChE Journal, 1997. **43** (3): p. 665-672.

23. Tien, C. and B.V. Ramarao, *Can filter cake porosity be estimated based on the Kozeny-Carman equation?* Powder Technology, 2013.**237** : p. 233-240.

24. Sorensen, P.B., P. Moldrup, and J.A.A. Hansen, *Filtration and expression of compressible cakes.* Chemical Engineering Science, 1996.**51** (6): p. 967-979.

25. Smiles, D.E., *Use of material coordinates in porous media solute and water flow.* Chemical Engineering Journal, 2000.**80** (1-3): p. 215-220.

26. Tosun, I., *Formulation of cake filtration.* Chemical Engineering Science, 1986. **41** (10): p. 2563-2568.

27. Meyer, B.A. and D.W. Smith, *Flow through porous media - Comparison of consolidated and unconsolidated materials.* Industrial & Engineering Chemistry Fundamentals, 1985. **24** (3): p. 360-368.

28. Andersen, N.P.R., M.L. Christensen, and K. Keiding, *New approach to determining consolidation coefficients using cake-filtration experiments.* Powder Technology, 2004. **142** (2-3): p. 98-102.

29. Hazelhoff Heeres, D.P., *Pressure filtration of milk fat slurries* , in *MSc thesis, Faculty of Applied Sciences, Department of Chemical Engineering* . 2018, Delft University of Technology: Delft.

30. Torquato, S., T.M. Truskett, and P.G. Debenedetti, *Is random close packing of spheres well defined?* Physical Review Letters, 2000.**84** (10): p. 2064-2067.